Infrared Spectra of the Sulfenic Ester CH_3SOCH_3 and Its Photodissociation Products in Solid Argon

Mohua Chen, Rongjing Yang, Renhu Ma, and Mingfei Zhou*

Department of Chemistry, Shanghai Key Laboratory of Molecular Catalysts and Innovative Materials, Advanced Materials Laboratory, Fudan University, Shanghai 200433, People's Republic of China

Received: April 21, 2008; Revised Manuscript Received: May 23, 2008

UV light irradiation of dimethyl sulfoxide (DMSO) in low temperature solid argon matrix produces sulfenic ester, CH_3SOCH_3, a high energy structural isomer of DMSO. The sulfenic ester molecule further dissociates to the CH_2O-CH_3SH complex under 266 nm laser irradiation. The CH_2S-CH_3OH complex is also formed upon UV light irradiation. The infrared spectra of the aforementioned species are assigned on the basis of isotopic substitutions (^{13}C and deuterium) as well as density functional frequency calculations.

Introduction

The photochemistry of sulfoxides has attracted considerable interest.[1,2] It is generally assumed that the photolysis mechanism of sulfoxides begins with homolytic cleavage of a C−S bond with the formation of the sulfenic ester. The observed photolysis end products are derived from the radical pair or biradical obtained by the secondary photolysis of the sulfenic ester, which resulted in the S−O bond cleavage (Scheme 1).

As compared to the related peroxides (ROOR′) and disulfides (RSSR′), the sulfenic esters are relatively uncommon. The structure and stability of many sulfenic esters have been studied. The relative stability between the sulfoxide and sulfenic ester structures depends on the nature of the substituent R. The sulfoxide structure is more stable than the sulfenic ester structure when R is an organic substituent. Several sulfenic esters have been prepared, and their structure and spectra were reported.[3–6] Recently, photoisomerization of matrix isolated bis(trifluoromethyl) sulfoxide was investigated. The sulfenic ester CF_3SOCF_3 was produced via photon-induced isomerization of $CF_3S(O)CF_3$ and is characterized spectroscopically.[7]

In this Article, we present an infrared spectroscopic study on the photoisomerization of matrix isolated dimethyl sulfoxide (DMSO). We will show that the simplest sulfenic ester CH_3SOCH_3 is formed via UV photon-induced isomerization of DMSO. The infrared absorption spectrum of CH_3SOCH_3 is obtained and assigned. In addition, the secondary photochemical products from sulfenic ester are also reported.

Experimental and Computational Methods

The experimental setup for matrix isolation infrared spectroscopic investigation has been described in detail previously.[8] Briefly, the DMSO/Ar mixture was deposited onto a CsI window cooled normally to 6 K by means of a closed-cycle helium refrigerator (ARS, 202N). The DMSO liquid was dried by calcium oxide, and the DMSO/Ar mixtures were prepared in a stainless steel vacuum line using standard manometric technique. In general, matrix samples were deposited for 1 h at a rate of approximately 4 mmol/h. Isotopic-labeled ^{13}DMSO (ISOTEC, 99%) and DMSO-d_6 (Aldrich, 99.96%) were used without further purification. The infrared absorption spectra of the resulting samples were recorded on a Bruker IFS 66V spectrometer at 0.5 cm^{-1} resolution between 4000 and 450 cm^{-1} using a liquid nitrogen cooled HgCdTe (MCT) detector. Matrix samples were subjected to photolysis using a high-pressure mercury lamp with glass filters or 266 nm UV laser light.

SCHEME 1

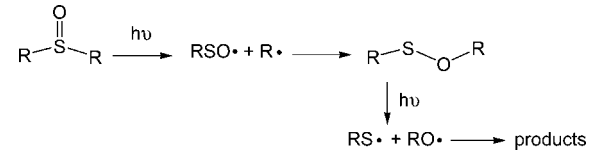

Quantum chemical calculations were performed using the Gaussian 03 program.[9] The three-parameter hybrid functional according to Becke with additional correlation corrections due to Lee, Yang, and Parr (B3LYP) was utilized.[10,11] The presence of a sulfur atom requires relatively larger basis sets, and the 6-311++G-(3df,3pd) basis set was used for the H, C, O, and S atoms. The geometries were fully optimized; the harmonic vibrational frequencies were calculated, and zero-point vibrational energies (ZPVE) were derived. Transition state optimizations were done with the synchronous transit-guided quasi-Newton (STQN) method[12] at the B3LYP/6-311++G(3df,3pd) level followed by the vibrational frequency calculations, showing the obtained structures to be true saddle points.

Results and Discussion

The infrared spectra of the photoreaction products are reported, and the product absorptions will be assigned by consideration of the frequencies and isotopic shifts and by comparisons with theoretical frequency calculations.

Infrared Spectra. The premixed $CH_3S(O)CH_3$/Ar mixture was deposited. The spectrum after sample deposition at 6 K without broadband irradiation shows the DMSO absorptions and trace of water absorptions.[13] When the as-deposited sample was subjected to broadband irradiation using a high pressure mercury arc lamp, new product absorptions were produced. The sample after broadband photolysis was subsequently subjected to secondary photolysis with 266 nm laser irradiation. The spectra in selected regions are shown in Figures 1–4, respectively. As shown in Figures 1–4, the DMSO absorptions decreased upon broadband irradiation, during which some new absorptions were produced. These product

* Corresponding author. E-mail: mfzhou@fudan.edu.cn.

10.1021/jp803436m CCC: $40.75
Published on Web 07/17/2008

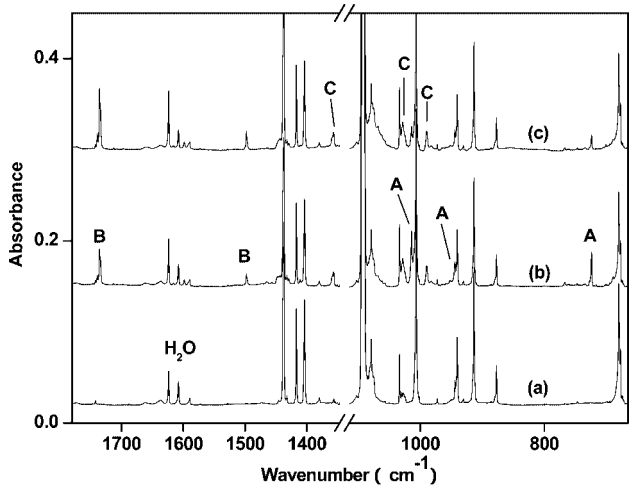

Figure 1. Infrared spectra in the 1780−1347 and 1115−665 cm^{-1} regions from deposition of 0.1% $CH_3S(O)CH_3$ in argon at 6 K. (a) After 1 h of sample deposition, (b) after 20 min of broadband irradiation ($250 < \lambda < 580$ nm), and (c) after additional 10 min of 266 nm laser irradiation.

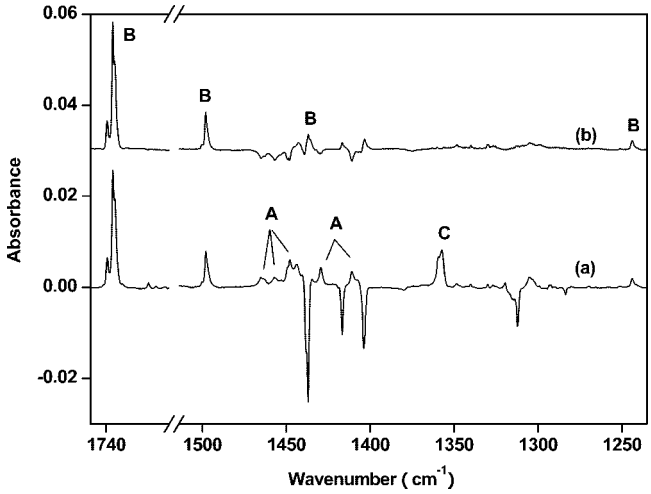

Figure 2. Difference IR spectra in the 1750−1700 and 1515−1235 cm^{-1} regions from deposition of 0.1% $CH_3S(O)CH_3$ in argon at 6 K. (a) Spectrum taken after 20 min of broadband photolysis minus spectrum taken after sample deposition without photolysis (absorptions pointing down are due to DMSO), and (b) spectrum taken after secondary 266 nm laser photolysis minus spectrum taken after 20 min of broadband photolysis (absorptions pointing down are due to product A).

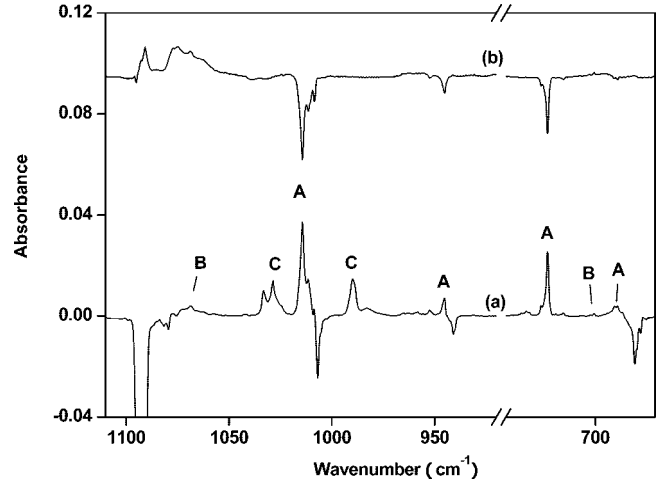

Figure 3. Difference IR spectra in the 1110−920 and 745−670 cm^{-1} regions from deposition of 0.1% $CH_3S(O)CH_3$ in argon at 6 K. (a) Spectrum taken after 20 min of broadband photolysis minus spectrum taken after sample deposition without photolysis (absorptions pointing down are due to DMSO), and (b) spectrum taken after secondary 266 nm laser photolysis minus spectrum taken after 20 min of broadband photolysis.

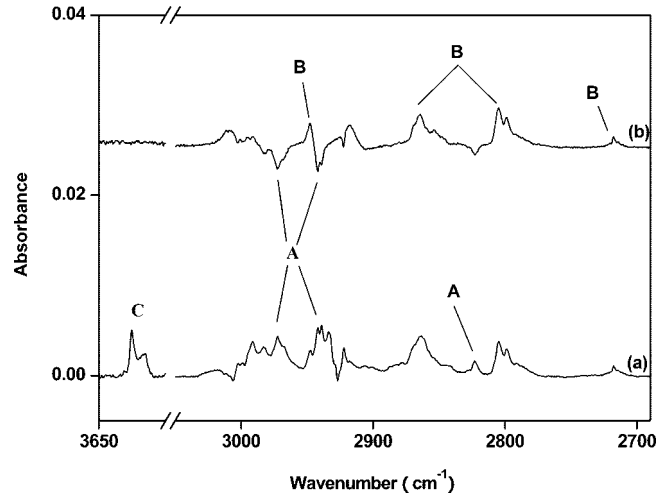

Figure 4. Difference IR spectra in the 3650−3600 and 3050−2700 cm^{-1} regions from deposition of 0.1% $CH_3S(O)CH_3$ in argon at 6 K. (a) Spectrum taken after 20 min of broadband photolysis minus spectrum taken after sample deposition without photolysis (absorptions pointing down are due to DMSO), and (b) spectrum taken after secondary 266 nm laser photolysis minus spectrum taken after 20 min of broadband photolysis.

absorptions can be classified into three groups on the basis of their behavior upon secondary photolysis with 266 nm laser light (groups A, B, and C hereafter, see Table 1). The group A absorptions decreased upon subsequent 266 nm laser irradiation, while the group B absorptions increased. The group C absorptions remain almost unchanged upon 266 nm laser irradiation.

Experiments were repeated with the isotopic-labeled $^{13}CH_3S(O)^{13}CH_3$ and $CD_3S(O)CD_3$ samples. The isotopic frequencies are also listed in Table 1.

CH_3SOCH_3. The group A absorptions maintain the same relative intensities throughout all of the experiments and are assigned to different vibrational modes of the sulfenic ester CH_3SOCH_3 in solid argon. The strongest absorption appeared at 1014.4 cm^{-1}. This position is in the region where the C−O single bond or the S═O double bond stretching vibrations should occur. It shifted to 998.2 cm^{-1} when the $^{13}CH_3S(O)^{13}CH_3$/Ar sample was used. The C-13 isotopic shift of 16.2 cm^{-1} ($^{12}C/^{13}C$ isotopic frequency ratio of 1.0162) indicates that this absorption is due to a C−O stretching vibration. The C−O stretching mode of CH_3OH is observed at 1034 cm^{-1} in solid argon, exhibiting an isotopic $^{12}C/^{13}C$ frequency ratio of 1.0150. The second strongest absorption of product A appeared at 724.1 cm^{-1}. This absorption shows small frequency shifts with C-13 and deuterium isotopic substitutions and is appropriate for the S−O stretching vibration. The S−O stretching modes of HSOH[14,15] and CF_3SOCF_3[7] isolated in solid argon are observed at 763.0 and 769.2 cm^{-1}, respectively. The third strongest absorption of product A has a band position at 945.3 cm^{-1}. This absorption shows $^{12}C/^{13}C$ and H/D isotopic frequency ratios of 1.0084 and 1.2251, respectively, and is assigned to the CH_3 rocking vibration of the sulfenic ester. Besides the aforementioned strong absorptions, weak absorptions at 2983.3, 2972.9, and 2942.1 cm^{-1} are assigned to the C−H stretching vibrations of the two CH_3 subunits (Table 1). The absorptions at 1465.2, 1457.2,

TABLE 1: Observed Infrared Absorptions (cm^{-1}) of the Photolysis Products of DMSO in Solid Argon

$CH_3S(O)CH_3$	$^{13}CH_3S(O)^{13}CH_3$	$CD_3S(O)CD_3$	266 nm[a]	assignment[b]
3626.1	3625.9	2677.8	—	C, ν(O−H)
2983.3	2972.7	2254.1	↓	A, $\nu^{as}(CH_3)$
2972.9	2962.8	2247.8	↓	A, $\nu^{as}(CH_3)$
2948.1	2943.1	2146.1	↑	B, $\nu^{as}(CH_3)$
2942.1	2936.6	2132.8	↓	A, $\nu^{s}(CH_3)$
2864.7	2846.9	2184.1	↑	B, $\nu^{as}(CH_2)$
2804.8	2801.1	2075.4	↑	B, $\nu^{s}(CH_2)$
2717.9	2708.4	1968.7	↑	B, $\delta(CH_2) + \rho(CH_2)$
1735.7	1698.2	1968.7	↑	B, ν(C═O)
1498.0	1498.0		↑	B, $\delta(CH_2)$
1465.2	1461.1	1064.2	↓	A, $\delta^{as}(CH_3)$
1457.2			↓	A, $\delta^{as}(CH_3)$
1448.2	1445.3	1056.8	↓	A, $\delta^{as}(CH_3)$
1443.4	1441.4	1047.0	↑	B, $\delta^{as}(CH_3)$
1429.6	1424.3	1101.5	↓	A, $\delta^{as}(CH_3)$
1411.1	1407.8	1029.5	↓	A, $\delta^{s}(CH_3)$
1357.3	1353.1		—	C, δ(COH)
1243.9	1235.0		↑	B, $\rho(CH_2)$
1068.8	1062.7	823.1	↑	B, δ(CSH)
1028.8	1008.8	960.6	—	C, ν(C−O)
1014.4	998.2	988.3	↓	A, ν(C−O)
		938.4	↓	A, $\rho(CH_3)$
		893.6	↓	A, $\rho(CH_3)$
990.0	978.6	797.3/795.4	—	C, $\omega(CH_2)$
945.3	937.5	772.0	↓	A, $\rho(CH_3)$
724.1	718.5	691.7	↓	A, ν(S−O)
700.3	685.5	670.2	↑	B, ν(C−S)
690.3	678.5	628.6	↓	A, ν(C−S)

[a] The intensities changed after the secondary 266 nm irradiation: ↑, growth; ↓, decrease; —, no change. [b] A, CH_3SOCH_3; B, CH_2O-CH_3SH; C, CH_2S-CH_3OH. ν, stretching; δ, bending; ρ, rocking; ω, wagging; and τ, torsion.

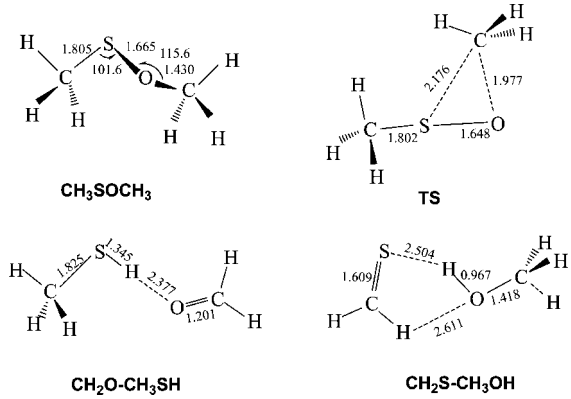

Figure 5. B3LYP/6-311++G(3df,3pd) optimized structures (bond lengths in Å, bond angles in deg) of the products from photoisomerization and dissociation of DMSO.

1448.2, 1429.6, and 1411.1 cm^{-1} are attributed to the CH_3 deformation modes.

To validate the experimental assignment and to obtain insight into the geometric structure of CH_3SOCH_3, we performed density functional theory calculations. The optimized structure is shown in Figure 5. Only the gauche conformation of CH_3SOCH_3 was predicted to be stable. The structure has a δ_{CSOC} dihedral angle of 88.9°, which lies between the δ_{COOC} of CH_3OOCH_3 at 119° and the δ_{CSSC} of CH_3SSCH_3 at around 84°.[16–18] The calculated vibrational frequencies and infrared intensities of CH_3SOCH_3 are listed in Table 2. The C−O stretching, S−O stretching, and the CH_3 rocking vibrations were predicted at 1023.9, 715.3, and 963.9 cm^{-1}, respectively. These three modes were predicted to have the largest IR intensities, which is in accord with the experimental observations. The experimental and calculated vibrational frequencies and isotopic frequency ratios are compared in Table 3. The calculated harmonic vibrational frequencies are slightly higher than the experimentally observed anharmonic frequencies except for the S−O and C−S stretching vibrations. The S−O and C−S stretching modes were predicted at 715.3 and 680.7 cm^{-1}, which are about 8.8 and 9.6 cm^{-1} lower than the frequencies observed in solid argon. Similar frequency underestimation has also been reported for CF_3SOCF_3[7] and some other sulfur-containing compounds.[19] As listed in Table 3, the calculated isotopic frequency ratios ($^{12}C/^{13}C$ and H/D) are in quite good agreement with the experimental values.

CH_2O-CH_3SH. The group B absorptions increased at the expense of the CH_3SOCH_3 absorptions under 266 nm laser irradiation. The most intense absorption at 1735.7 cm^{-1} shifted to 1698.2 cm^{-1} with the $^{13}CH_3S(O)^{13}CH_3$ sample. The band position and isotopic frequency ratio (1.0221) suggest that this absorption is due to a C═O stretching mode, and the band position is very close to that of CH_2O in solid argon (1742 cm^{-1}).[20] The band positions of the 2864.7, 2804.8, 1498.0, and 1243.9 cm^{-1} absorptions are also very close to those of CH_2O absorptions at 2863, 2797.1, 1498.8, and 1244.8 cm^{-1} in solid argon. These observations indicate that product B involves a CH_2O fragment and most likely is due to a CH_2O-X complex. Because the group B absorptions increased at the expense of the CH_3SOCH_3 absorptions, this indicates that product B should be a photodissociation product of CH_3SOCH_3. Therefore, the X fragment is assumed to be CH_3SH. The weak absorptions at 2948.1, 1443.4, and 700.3 cm^{-1} are due to the C−H stretching, CH_3 deformation, and C−S stretching modes of the CH_3SH fragment in the CH_2O-CH_3SH complex. The strongest absorption of CH_3SH isolated in solid argon is the S−C stretching mode. This mode is observed at 704 cm^{-1},[21] only several wavenumbers above the 700.3 cm^{-1} absorption. A weak absorption at 2717.9 cm^{-1} is due to the combination mode of the CH_2O fragment (CH_2 bending plus CH_2 rocking). The same combination mode of the previously reported CH_2O-HNO complex was observed at 2720 cm^{-1}.[22] In a recently reported photoisomerization study of $CF_3S(O)CF_3$, both the CF_2O and the CF_3SF fragments were observed to be the secondary photolysis products of CF_3SOCF_3.[7]

The CH_2O-CH_3SH complex was predicted to have a nonplanar structure with the O atom of the CH_2O fragment coordinated to the sulfhydryl hydrogen atom of the CH_3SH subunit (Figure 5). The O−H distance was predicted to be 2.377 Å, which indicates a weak interaction between CH_2O and CH_3SH. As listed in Table 2, the calculated frequencies are in reasonable agreement with the observed values. The ν(C═O) and $\delta(CH_2)$ frequencies of CH_2O were predicted to be red-shifted by 9.9 and 2.4 cm^{-1} upon CH_3SH coordination, only slightly larger than the observed shifts of 6.3 and 0.8 cm^{-1}.

CH_2S-CH_3OH. The group C absorptions are assigned to the CH_2S-CH_3OH complex. The 3626.1, 1357.3, and 1028.8 cm^{-1} absorptions are due to the O−H stretching (ν(O−H)), HOC bending (δ(COH)), and C−O stretching (ν(C−O)) vibrations of the CH_3OH subunit. The O−H stretching and C−O stretching modes are red-shifted by 41.2 and 5.2 cm^{-1}, whereas the HOC bending mode is blue-shifted by 22.3 cm^{-1} with respect to the corresponding absorptions of CH_3OH isolated in solid argon (3667.3, 1335, and 1034.0 cm^{-1}). The 990.0 cm^{-1} absorption is very close to the CH_2 wagging vibration ($\omega(CH_2)$) of CH_2S in solid argon reported at 987.4 cm^{-1},[23] which is the strongest absorption of CH_2S. As a reference point, the CH_2 wagging vibration of the CH_2S-HCl complex was observed at 994.1 cm^{-1}.[24] The acidity of CH_3OH is weaker than that of

TABLE 2: Calculated Total Energies (in Hartree, after Zero Point Energy Corrections), Vibrational Frequencies (cm^{-1}), and Intensities (km/mol) of DMSO and Its Photolysis Products at the B3LYP/6-311++G(3df,3dp) Level

molecule	energy	frequency (intensity)
$CH_3S(O)CH_3$	−553.22721	3144.5(3); 3144.0(1);3136.7(10); 3132.2(0); 3039.5(7); 3037.2(4); 1476.5(17); 1458.6(0); 1456.0(5); 1442.2(9); 1336.3(10); 1316.6(1); 1109.0(146); 1024.7(15); 956.5(8); 927.3(8); 889.5(2); 665.3(17); 636.9(8); 368.9(7); 319.6(8); 282.7(0); 231.5(0); 189.1(0)
CH_3SOCH_3	−553.22064	3121.2(7); 3113.3(18); 3110.0(10); 3080.5(33); 3031.1(16); 3014.2(49); 1498.9(10); 1487.3(7); 1480.2(11); 1466.8(2); 1448.8(7); 1341.7(0); 1192.4(2); 1171.5(2); 1023.9(108); 968.5(2); 963.9(15); 715.3(39); 680.7(5); 371.4(2); 302.3(5); 177.7(1); 166.3(1); 98.8(2)
CH_2O-CH_3SH	−553.23240	3136.7(6); 3134.4(6); 3052.9(26); 2967.4(97); 2899.3(68); 2652.6(37); 1811.4(97); 1528.7(20); 1489.4(7); 1475.8(4); 1360.7(5); 1269.4(9); 1207.9(5); 1107.9(13); 973.7(4); 820.0(1); 701.5(2); 347.7(20); 134.8(0); 116.4(8); 86.1(10); 54.8(10); 43.4(19); 28.2(4)
CH_2S-CH_3OH	−553.21397	3709.1(327); 3168.9(1); 3103.7(31); 3075.2(21); 3036.7(54); 2990.8(79); 1510.7(3); 1497.6(3); 1493.0(2); 1479.3(5); 1399.3(64); 1174.3(1); 1107.2(14); 1085.1(14); 1057.1(133); 1047.9(36); 1015.2(9); 501.6(84); 219.9(1); 146.3(2); 105.5(0); 90.5(1); 59.6(20); 22.9(8)

TABLE 3: Comparison of the Observed and Calculated Vibrational Frequencies (cm^{-1}) and Isotopic Frequency Ratios of the Observed Products

		freq.		$^{12}C/^{13}C$		H/D	
molecule	mode	obs.	calc.	obs.	calc.	obs.	calc.
CH_3SOCH_3	$\nu^{as}(CH_3)$	2983.3	3110.0	1.0037	1.0036	1.3235	1.3478
	$\nu^{as}(CH_3)$	2972.9	3080.5	1.0034	1.0037	1.3226	1.3475
	$\nu^{s}(CH_3)$	2942.1	3014.2	1.0018	1.0009	1.3795	1.3971
	$\delta^{as}(CH_3)$	1465.2	1498.9	1.0028	1.0015	1.3768	1.3844
	$\delta^{as}(CH_3)$	1457.2	1487.3		1.0018		1.3824
	$\delta^{as}(CH_3)$	1448.2	1480.2	1.0020	1.0018	1.3704	1.3776
	$\delta^{s}(CH_3)$	1429.6	1466.8	1.0040	1.0036	1.2980	1.3086
	$\delta^{as}(CH_3)$	1411.1	1448.8	1.0021	1.0019	1.3707	1.3827
	$\nu(C-O)$	1014.4	1023.9	1.0162	1.0169	1.0264	1.0263
	$\rho(CH_3)$	945.3	963.9	1.0084	1.0086	1.2251	1.2364
	$\nu(S-O)$	724.1	715.3	1.0079	1.0070	1.0468	1.0441
	$\nu(C-S)$	690.3	680.7	1.0178	1.0187	1.0982	1.0956
CH_2O-CH_3SH	$\nu^{as}(CH_3)$	2947.6	3052.9	1.0017	1.0009	1.3737	1.3970
	$\nu^{as}(CH_2)$	2864.7	2967.4	1.0063	1.0043	1.3116	1.3389
	$\nu^{s}(CH_2)$	2804.8	2899.3	1.0015	1.0014	1.3520	1.3708
	$\nu(C=O)$	1735.7	1811.4	1.0222	1.0226	1.0273	1.0277
	$\delta(CH_2)$	1498.0	1528.7	1.0000	1.0001		1.3732
	$\delta^{as}(CH_3)$	1443.4	1489.4	1.0014	1.0017	1.3786	1.3821
	$\rho(CH_2)$	1243.9	1269.4	1.0076	1.0077		1.2666
	$\delta(CSH)$	1068.8	1107.9	1.0056	1.0056	1.2984	1.3121
	$\nu(C-S)$	700.3	701.5	1.0216	1.0231	1.0449	1.0498
CH_2S-CH_3OH	$\nu(O-H)$	3626.1	3709.1	1.0001	1.0000	1.3546	1.3727
	$\delta(COH)$	1357.3	1399.3	1.0033	1.0049		1.2750
	$\nu(C-O)$	1028.8	1057.0	1.0194	1.0173	1.0702	1.0637
	$\omega(CH_2)$	990.0	1047.9	1.0113	1.0096	1.2447	1.2710

HCl; therefore, the interaction between CH_2S and CH_3OH is considered to be weaker than that in the CH_2S-HCl complex, which results in a smaller shift of the CH_2 wagging vibration in CH_2S-CH_3OH than that in CH_2S-HCl.

DFT/B3LYP calculations were performed on the CH_2S-CH_3OH complex. As shown in Figure 5, the complex involves a five-membered ring structure with the S atom of the CH_2S fragment coordinated to the hydroxyl hydrogen atom of the CH_3OH fragment with a S−H distance of 2.504 Å, while the oxygen atom of CH_3OH is also weakly interacting with one of the hydrogen atom of CH_2S with an O−H distance of 2.611 Å. The calculated frequencies and relative intensities of the CH_2S-CH_3OH complex match the experimental values very well (Table 3).

Reaction Mechanism. The photochemistry of sulfoxides has been the subject of many previous investigations.[2] The initial step of the photolysis process is generally assumed to be the cleavage of a C−S bond of sulfoxide with the formation of the sulfenic ester intermediate. The CH_3SOCH_3 structure is predicted to be 4.3 kcal/mol higher in energy than the $CH_3S(O)CH_3$ structure at the B3LYP/6-311++G(3df,3pd) level of theory, which is consistent with the relative stability calculated by Jenks et al. using the G2 method.[25] Therefore, the isomerization reaction is slightly endothermic. In the $CF_3S(O)CF_3-CF_3SOCF_3$ system, the sulfenic ester form was predicted to be more stable than the sulfoxide structure due to the strong electron-withdrawing CF_3 unit.[7] According to theoretical calculations, there are two possible mechanisms from sulfoxide to sulfenic ester as shown in Figure 6. The first path is methyl group migration from S to O to give CH_3SOCH_3 via a transition state, which lies about 74.0 kcal/mol above $CH_3S(O)CH_3$. The second path

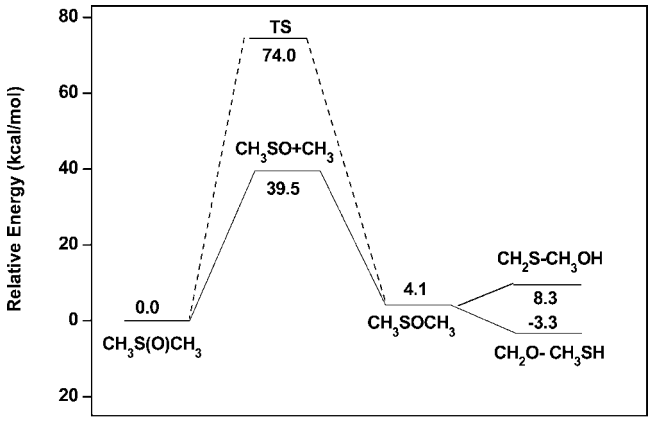

Figure 6. B3LYP/6-311++G(3df,3pd) calculated energy profiles for the isomerization and dissociation reactions of DMSO. (Energies are given in kcal/mol and are relative to the ground state of DMSO).

proceeds with the formation of the CH_3SO and CH_3 radical pair by cleavage of one C−S bond of $CH_3S(O)CH_3$ followed by radical recombination. The C−S bond cleavage requires 39.5 kcal/mol energy. Apparently, the second path is dynamically more favorable than the first path. In the previous studies on the photolysis of sulfoxides in solutions, the sulfoxide to sulfenic ester reactions were suggested to proceed via the C−S cleavage mechanism. In the present experiments, the CH_3SOCH_3 absorptions were produced upon broadband irradiation of $CH_3S(O)CH_3$ isolated in solid argon. Filtered experiment with high pressure mercury arc lamp indicates that only the light in the wavelength range of 250−300 nm is responsible for the photochemistry of $CH_3S(O)CH_3$ in solid argon. No photolysis products were observed after 266 nm laser irradiation of the as-deposited $CH_3S(O)CH_3$/Ar sample. These observations suggest that the light with wavelength shorter than 266 nm plays a major role in the photochemical process. The photon energy in this wavelength range is sufficient to overcome the energy barriers for both reaction paths from $CH_3S(O)CH_3$ to CH_3SOCH_3.

During broadband irradiation of $CH_3S(O)CH_3$, both the CH_2O-CH_3SH and the CH_2S-CH_3OH complexes were also formed. The CH_2O-CH_3SH complex absorptions increased at the expense of the CH_3SOCH_3 absorptions upon the secondary irradiation with 266 nm laser light. The direct photolysis of $CH_3S(O)CH_3$ under 266 nm laser light failed to produce any product absorptions, which suggests that the CH_2O-CH_3SH and CH_2S-CH_3OH complexes are formed by the secondary photolysis of the CH_3SOCH_3 intermediates. The complexes are assumed to be derived from the radical pair obtained by cleavage of the S−O bond of sulfenic ester.[26] Although the S−O bond is stronger than the C−O band as calculated by Jenks et al.,[25] only S−O bond cleavage was observed experimentally. The in situ formed CH_3S and CH_3O radicals cannot escape the matrix cage and form the CH_2O-CH_3SH and CH_2S-CH_3OH complexes via different hydrogen atom transfer processes. According to calculations at the B3LYP/6-311++G(3df,3pd) level, the CH_2O-CH_3SH complex is 7.4 kcal/mol lower in energy than CH_3SOCH_3, whereas the CH_2S-CH_3OH complex lies 4.2 kcal/mol above CH_3SOCH_3. Experimentally, only the CH_2O-CH_3SH complex was produced upon secondary photolysis of CH_3SOCH_3 with 266 nm laser light.

Conclusions

Dimethyl sulfoxide (DMSO) has been found to undergo photoisomerization to the sulfenic ester, CH_3SOCH_3, under UV light irradiation in solid argon. Density functional calculations predicted that the sulfenic ester has only one stable gauche conformation, which is slightly less stable than the dimethyl sulfoxide isomer. It is found that the sulfenic ester further dissociates to the CH_2O-CH_3SH complex under 266 nm laser irradiation. The CH_2S-CH_3OH complex is also formed upon UV light irradiation. The infrared spectra of the aforementioned species are assigned on the basis of isotopic substitutions (^{13}C and deuterium) as well as density functional frequency calculations.

Acknowledgment. This work is supported by the NKBRSF (2007CB815203) and NNSFC (20773030 and 20433080) of China.

References and Notes

(1) Still, I. W. J. In *The Chemistry of Sulfones and Sulfoxides*; Patai, S., Rappaport, Z., Stirling, C. J. M., Eds.; John Wiley & Sons Ltd.: New York, 1988; pp 873−887.

(2) (a) Guo, Y.; Jenks, W. S. *J. Org. Chem.* **1997**, *62*, 857. (b) Guo, Y.; Jenks, W. S. *J. Org. Chem.* **1995**, *60*, 5480.

(3) Miller, E. G.; Rayner, D. R.; Thomas, H. T.; Mislow, K. *J. Am. Chem. Soc.* **1968**, *90*, 4861.

(4) Wolfe, S.; Schlegel, H. B. *Gazz. Chim. Ital.* **1990**, *120*, 285.

(5) (a) Baumeister, E.; Oberhammer, H.; Schmidt, H.; Steudel, R. *Heteroat. Chem.* **1991**, *2*, 633. (b) Steudel, R.; Schmidt, H.; Baumeister, E.; Oberhammer, H.; Koritsanszky, T. *J. Phys. Chem.* **1995**, *99*, 8987. (c) Ulic, S. E.; Della Védova, C. O.; Hermann, A.; Mack, H. G.; Oberhammer, H. *Inorg. Chem.* **2002**, *41*, 5699. (d) Ulic, S. E.; Kosma, A.; Leibold, C.; Della Védova, C. O.; Willner, H.; Oberhammer, H. *J. Phys. Chem. A* **2005**, *109*, 3739.

(6) Du, L.; Yao, L.; Zeng, X. Q.; Ge, M. F.; Wang, D. X. *J. Phys. Chem. A* **2007**, *111*, 4944.

(7) Ulic, S. E.; Ahsen, S. V.; Willner, H. *Inorg. Chem.* **2004**, *43*, 5268.

(8) Wang, G. J.; Zhou, M. F. *Int. Rev. Phys. Chem.* **2008**, *27*, 1.

(9) Frisch, M. J.; Trucks, G. W.; Schlegel, H. B.; Scuseria, G. E.; Robb, M. A.; Cheeseman, J. R.; Montgomery, J. A., Jr.; Vreven, T.; Kudin, K. N.; Burant, J. C.; Millam, J. M.; Iyengar, S. S.; Tomasi, J.; Barone, V.; Mennucci, B.; Cossi, M.; Scalmani, G.; Rega, N.; Petersson, G. A.; Nakatsuji, H.; Hada, M.; Ehara, M.; Toyota, K.; Fukuda, R.; Hasegawa, J.; Ishida, M.; Nakajima, T.; Honda, Y.; Kitao, O.; Nakai, H.; Klene, M.; Li, X.; Knox, J. E.; Hratchian, H. P.; Cross, J. B.; Adamo, C.; Jaramillo, J.; Gomperts, R.; Stratmann, R. E.; Yazyev, O.; Austin, A. J.; Cammi, R.; Pomelli, C.; Ochterski, J. W.; Ayala, P. Y.; Morokuma, K.; Voth, G. A.; Salvador, P.; Dannenberg, J. J.; Zakrzewski, V. G.; Dapprich, S.; Daniels, A. D.; Strain, M. C.; Farkas, O.; Malick, D. K.; Rabuck, A. D.; Raghavachari, K.; Foresman, J. B.; Ortiz, J. V.; Cui, Q.; Baboul, A. G.; Clifford, S.; Cioslowski, J.; Stefanov, B. B.; Liu, G.; Liashenko, A.; Piskorz, P.; Komaromi, I.; Martin, R. L.; Fox, D. J.; Keith, T.; Al-Laham, M. A.; Peng, C. Y.; Nanayakkara, A.; Challacombe, M.; Gill, P. M. W.; Johnson, B.; Chen, W.; Wong, M. W.; Gonzalez, C.; Pople, J. A. Gaussian 03, revision B.05; Gaussian, Inc.: Pittsburgh, PA, 2003.

(10) Becke, A. D. *J. Chem. Phys.* **1993**, *98*, 5648.

(11) Lee, C.; Yang, W.; Parr, R. G. *Phys. Rev. B* **1988**, *37*, 785.

(12) Head-Gordon, M.; Pople, J. A.; Frisch, M. *Chem. Phys. Lett.* **1988**, *153*, 503.

(13) Barnes, A. J.; Wright, M. P. *J. Chem. Soc., Faraday Trans II.* **1986**, *82*, 165.

(14) Smardzewski, R. R.; Lin, M. C. *J. Chem. Phys.* **1977**, *66*, 3197.

(15) Beckers, H.; Esser, S.; Metzroth, T.; Behnke, M.; Willner, H.; Gauss, J.; Hahn, J. *Chem.-Eur. J.* **2006**, *12*, 832.

(16) Haas, B.; Oberhammer, H. *J. Am. Chem. Soc.* **1984**, *106*, 6146.

(17) Sutter, D.; Dreizler, H.; Rudolph, F. *Z. Naturforsch.* **1964**, *19*, 512.

(18) Beagly, B.; McAloon, K. T. *Trans. Faraday Soc.* **1971**, *67*, 3216.

(19) Zeng, A. H.; Yu, L.; Wang, Y.; Kong, Q. Y.; Xu, Q.; Zhou, M. F. *J. Phys. Chem. A* **2004**, *108*, 6656.

(20) Khoshkoo, H.; Nixon, E. R. *Spectrochim. Acta* **1973**, *29A*, 603.

(21) Barnes, A. J.; Hallam, H. E.; Howells, J. D. R. *J. Chem. Soc., Faraday Trans. 2* **1972**, *68*, 737.

(22) Müller, R. P.; Russegger, P.; Huber, J. R. *Chem. Phys.* **1982**, *70*, 281.

(23) Suzuki, E.; Yamazaki, M.; Shimizu, K. *Vib. Spectrosc.* **2007**, *43*, 269.

(24) Suzuki, E.; Yamazaki, M.; Shimizu, K. *J. Mol. Struct.* **2006**, *797*, 121.

(25) Gregory, D. D.; Jenks, W. S. *J. Org. Chem.* **1998**, *63*, 3859.

(26) (a) Pasto, D. J.; Hermine, G. L. *J. Org. Chem.* **1990**, *55*, 5815. (b) Pasto, D. J.; Cottard, F. *Tetrahedron Lett.* **1994**, *35*, 4303.

JP803436M